PHYSICAL REVIEW B VOLUME 8, NUMBER 10 15 NOVEMBER 1973

Inelastic Effects in Photoemission: Microscopic Formulation and Qualitative Discussion

C. Caroli, D. Lederer-Rozenblatt, B. Roulet, and D. Saint-James

Laboratoire de Physique des Solides de l'E.N.S. associé au centre National de la Recherche Scientifique Université, Paris VII, 2 place Jussieu, 75221 Paris Cedex 05, France

(Received 7 May 1973)

The previous microcoscopic models of photoemission are developed and reformulated in order to include inelastic scattering effects. A general expression is given for the photocurrent and its energy distribution (EDC). The problem of inelastic scattering is more thoroughly discussed in the case of electron-phonon interaction for a pseudo-one-dimensional model. The approximations necessary for a random-walk description of the propagation of the electron in the final state to be valid are given. The microscopic formulation is then used to discuss phenomenological models such as the step model. It is shown that, in general, this model is not a good picture since one cannot separate simply the optical-transition step from the propagation of the excited electron and its escaping into the vacuum. In particular, even in the absence of inelastic effects, it is impossible to make a general prediction about the degree of accuracy with which the EDC may reproduce the optical joint density of states of the semi-infinite solid. Finally the paper discusses what type of information about the solid may be reasonably extracted from EDC measurements as a function of the energy of the primary excited state. It is concluded that the best conditions are met for uv and x-ray photoemission for which the elastic EDC should give information about the occupied surface states (uv) and bulk density of states (x ray).

I. INTRODUCTION

Inelastic scattering plays a very important part in photoemission from solids. Indeed, since electrons have to escape into the vacuum in order to contribute to the photocurrent, the only transitions of interest in photoemission experiments are those in which the photon field excites electrons up to energies ω above the vacuum level. That is, $\omega - \mu > \phi$, where μ is the Fermi level of the solid and ϕ is its work function (typically $\phi \sim 4$ eV).

At such excitation energies, an electron in a semiconductor or a metal has a rather short mean free path (typically $\lesssim 100$ Å), even in impurity-free materials. In other words, scattering in the excited final state is non-negligible. It may originate from various mechanisms (electron-electron, electron-phonon, electron-impurity, etc. interactions), most of which involve inelastic processes. The relative importance of these mechanisms depends on the nature and purity of the material and on the final-state energy. For example, in a semiconductor, if $\omega - E_c < W_{eh}$ (where E_c is the bottom level of the conduction band and W_{eh} the minimum energy for creation of an electron-hole pair), electron-electron scattering does not contribute to energy losses. In a metal excited by uv light, if $\omega - \mu \sim 20$ eV the electron-electron mechanism dominates, etc. Inelastic processes give rise to the inelastic current (i.e., to electrons which have lost energy by creating some excitations of the solid before escaping) and to the finite extraction depth of the current (photoelectrons come from a finite layer along the surface). It is therefore necessary to take them into account, at least qualitatively, when interpreting experimental results.

There exist presently two types of theoretical approaches to photoemission:

(i) Semiphenomenological theories, which are founded on the so-called "three-steps model" originally put forward by Spicer.[1] In this model photoemission is decomposed into three independent processes—photoabsorption, propagation of the excited electron to the surface, escape into the vacuum. The first process is quantum mechanical and involves calculating optical joint density of states (for the initial and final electronic levels) in specific materials. In that step, inelastic scattering effects are usually neglected. The propagation process has been treated in the frame of quasiclassical random-walk models in one[2] and three dimensions.[3] The existing models deal essentially with inelastic scattering by phonons[4]; electron-electron losses are estimated qualitatively from approximate microscopic calculations of inelastic scattering cross sections.

(ii) The recent theories of Schaich and Ashcroft[5,6] and of Mahan[7] have given a complete microscopic formulation of the photoemission process in the absence of scattering, i.e., for an electron gas in the presence of a one-electron lattice potential. Scattering only appears via the introduction of a mean free path in the excited state in the final result for the current—which is therefore bound to be elastic. Langreth[8] has generalized such a microscopic theory to the case of elastic scattering by impurities.

It is not very clear at that stage how the two types of theories overlap or what is the degree of validity of the step picture. Comparing the two

approaches is of interest, since experimental results are most often analyzed with the help of the step model, owing to the complexity of the photoemission problem. Indeed, a complete quantitative *ab initio* theory must include, at the same time, the three-dimensional lattice structure, the breaking of symmetry due to the surface, with appearance of surface states, and the scattering effects.

In this paper we develop previous microscopic models so as to include inelastic scattering (Sec. II). We obtain a general expression for the photocurrent and its energy distribution (EDC). In Sec. III, we specialize to the case of electron-phonon interaction in a pseudo-one-dimensional metal, and show what approximations are necessary for a random-walk description of propagation in the final state to be valid. The problem is solved, in these approximations, for a free-electron conduction band plus step surface potential model.

On the basis of the microscopic analysis, Sec. IV first discusses the validity of the step model. It is shown to be, in general, not a good picture, because it does not properly include scattering effects and because, even when these effects are neglected, one cannot separate simply the "optical-transition step" from the two other ones. We then discuss qualitatively what kind of information about the emitting solid can be obtained from EDC measurements, as a function of the energy of the primary excited state. It is found that the best conditions are met in far-uv and x-ray photoemission, which should permit us to probe with a reasonable accuracy, respectively, the densities of surface and bulk initial states.

II. GENERAL EXPRESSION OF THE PHOTOCURRENT

Our approach is based on Keldysh's formalism for out-of-equilibrium many-body systems.[9] As will be clear in the following, this approach leads in the present problem, as it should, to the same formal results as the quadratic-response theory of Schaich and Ashcroft.[5] It is our opinion that it has the advantage of giving very systematic prescriptions for the calculation of the needed quadratic-response function in the presence of interactions. Moreover, it can be extended to true nonequilibrium situations such as photoassisted field emission.

Let us consider a semi-infinite solid at zero temperature, extending in the region $x<0$, with a perfectly flat surface at $x=0$, and let us call H_0 the Hamiltonian of electrons in this system (including, in particular, interactions between electrons and with phonons). The system is submitted to an electromagnetic field deriving from the vector potential

$$\vec{A}(\vec{r},t)=\hat{y}a(x)\cos\Omega t, \tag{1}$$

i.e., we choose the gauge so that the scalar potential is zero, and we assume the field to be monochromatic, linearly polarized along direction $\hat{y}$ parallel to the surface, and at normal incidence. $a(x)$ is oscillating in the vacuum ($x>0$), and decreases on a penetration depth δ in the solid ($x<0$). Moreover, we assume the solid to have complete translational invariance in the plane of the surface.[10]

The coupling between the field and the electrons is described by the Hamiltonian

$$H_1=\int d^3r\,\psi^\dagger(\vec{r},t)\times\left(\frac{ie\hbar}{mc}\vec{A}(\vec{r},t)\cdot\vec{\nabla}+\frac{e^2}{2mc^2}[\vec{A}(\vec{r},t)]^2\right)\psi(\vec{r},t), \tag{2}$$

where $\psi^\dagger$ and ψ are electron creation and destruction operators.

The total current density induced by the field is given (for the two spin directions[11]) by

$$\vec{j}(\vec{r},t)=2\hbar\left(\frac{e\hbar}{2m}(\vec{\nabla}_{r'}-\vec{\nabla}_r)+\frac{ie^2\vec{A}(\vec{r},t)}{mc}\right)\times G^+_{\rm tot}(\vec{r}t,\vec{r}'t)\,|_{\vec{r}'=\vec{r}}. \tag{3}$$

The "electron-occupation propagator" $G^+_{\rm tot}(\vec{r}t,\vec{r}'t')=i\langle\psi^\dagger(\vec{r}'t')\psi(\vec{r}t)\rangle$ is the first-row, second-column element of the Keldysh Green's-function matrix $\hat{G}_{\rm tot}$ of the solid in the presence of the field[9]

$$\hat{G}_{\rm tot}=\begin{pmatrix}G^c_{\rm tot} & G^+_{\rm tot}\\ G^-_{\rm tot} & \tilde{G}^c_{\rm tot}\end{pmatrix} \tag{4}$$

$G^c_{\rm tot}$ and $\tilde{G}^c_{\rm tot}$ are, respectively, the corresponding causal and anticausal functions, $G^-_{\rm tot}$ is the "hole-occupation propagator,"[12] and $G^+_{\rm tot}$, and therefore $\vec{J}$, can be expanded in powers of the field

$$G^+_{\rm tot}=G^+ + G^{(1)+}+G^{(2)+}+\cdots. \tag{5}$$

The first-order term in the expansion of $\vec{J}$ simply gives the linear conductivity current, which flows along $\hat{y}$ and is of no interest to us here. The photocurrent is given, to lowest order, by the term in $\vec{J}$ which is quadratic in $\vec{A}$ (i.e., linear in the number of photons). This term itself decomposes into two parts: (a) $\vec{A}G^{(1)+}(\vec{r}t,\vec{r}t)$, which is zero because of the rotational symmetry of the field-free system about the $\hat{x}$ axis (and in any case would not go out of the solid); (b) the only remaining term is

$$\vec{J}(\vec{r},t)=\frac{e\hbar^2}{m}(\vec{\nabla}_{r'}-\vec{\nabla}_r)G^{(2)+}(\vec{r}t,\vec{r}'t)\,|_{\vec{r}'=\vec{r}}. \tag{6}$$

Finally, photoemission experiments only measure the dc part of the total current flowing out of the whole surface; that is,

$$\langle J_x\rangle=\int\frac{d\omega}{2\pi}\int\frac{d^2k}{(2\pi)^2}$$

$$\times \frac{e\hbar^2}{m}\left(\frac{\partial}{\partial x'} - \frac{\partial}{\partial x}\right) G^{(2)+}_{\vec{k}\omega}(x, x') \Big|_{x'=x}, \qquad (7)$$

with

$$G^{(2)+}_{\vec{k}\omega}(x, x') = G^{(2)+}_{\vec{k}}(x, x';\ \omega, \omega') \Big|_{\omega'=\omega}$$

and

$$G^{(2)+}_{\vec{k}}(x, x';\ \omega, \omega') = \int d^2\vec{\rho}\, dt\, d^2\vec{\rho}'\, dt'\, G^{(2)+}(\vec{r}\, t,\ \vec{r}'t') \times \exp[i\vec{k}\cdot(\vec{\rho}-\vec{\rho}') - (\omega t - \omega' t')]. \qquad (8)$$

$\vec{\rho} = (y, z)$ is a vector lying in a plane parallel to the surface.

We must now calculate $G^{(2)+}_{\vec{k}\omega}$ by means of the Keldysh perturbation expansion. For the sake of clarity, we shall first perform the calculation for a system without interactions, then extend it to the interacting case.

A. Noninteracting System

$G^{(2)+}_{\vec{k}\omega}(x, x')$ is the term proportional to a^2 in the expansion of $\hat{G}^+$. It therefore contains two contributions, obtained, respectively, by treating the paramagnetic part of H_1 ($\sim \vec{A}\cdot\vec{\nabla}$) to second order and the diamagnetic part ($\sim A^2$) to first order.

H_1 is a one-body instantaneous perturbation, so the associated Keldysh self-energy matrix σ is simply proportional to[12]

$$\hat{\sigma}_z = \begin{pmatrix} 1 & 0 \\ 0 & -1 \end{pmatrix}.$$

Developing the matrix Dyson equation

$$\hat{G}_{\text{tot}} = \hat{G} + \hat{G}\,\hat{\sigma}\,\hat{G}_{\text{tot}}, \qquad (9)$$

we obtain

$$G^{(2)+}_{\vec{k}\omega}(x, x') = \int dx_1 \frac{e^2 a^2(x_1)}{4mc^2}\{\hat{G}_{\vec{k}\omega}(x, x_1)\hat{\sigma}_z\hat{G}_{\vec{k}\omega}(x_1, x')\}^+ + \frac{e^2\hbar^2 k_y^2}{4m^2c^2}\int dx_1 dx_2 a(x_1)a(x_2) \times \{\hat{G}_{\vec{k}\omega}(x, x_1)\hat{\sigma}_z[\hat{G}_{\vec{k},\omega+\Omega}(x_1, x_2) + \hat{G}_{\vec{k},\omega-\Omega}(x_1, x_2)]\hat{\sigma}_z\hat{G}_{\vec{k}\omega}(x_2, x')\}^+, \qquad (10)$$

where the subscript + means the first-row, second-column element of the result of the matrix products written between the { }. Carrying out the matrix products in Eq. (10), one finds that the diamagnetic contribution to the right-hand side can be written as

$$G^r_{\vec{k}\omega}(x, x_1)G^+_{\vec{k}\omega}(x_1, x') + G^+_{\vec{k}\omega}(x, x_1)G^a_{\vec{k}\omega}(x_1, x'), \qquad (11)$$

where G^a and G^r are the standard advanced and retarded propagators, which are analytic, respectively, in the lower- and upper-half ω planes.

Let us now examine the general properties of the propagators G of the solid-plus-vacuum system:

(a) By definition

$$G^+_{\vec{k}\omega}(x_1, x_2) = -2i\ \text{Im}\, G^r_{\vec{k}\omega}(x_1, x_2)\,\theta(\mu - \omega), \qquad (12)$$

with

$$\theta(x) = \begin{cases} 1, & \text{for } x > 0 \\ 0, & \text{for } x < 0 \end{cases}$$

and μ is the chemical potential of the system (i.e., G^+ describes properties of occupied electron states).

(b) E being the vacuum level (i.e., the potential felt by an electron at $x \to +\infty$), whatever the detailed shape of the potential created by the solid—including image-force effects—, one has

$$\lim_{x\to+\infty} \hat{G}_{k\omega}(x, x_1) = 0, \quad \text{if } \omega - \epsilon_k < E$$

where $\epsilon_k = \hbar^2k^2/2m$ is the part of the electron energy corresponding to motion parallel to the surface. In other words, an electron cannot escape if its transverse energy does not exceed the vacuum level.

If $\omega - \epsilon_k > E$, when $x \to \infty$ the elements of $\hat{G}_{\vec{k}\omega}(x, x_1)$'s are oscillating functions of x, the amplitudes of which depend on the details of the potential.

Since $\langle J_x \rangle$ is position independent, it can be calculated on any plane $x = cst$. It is clear from the above remark that it is most simple to do it at infinity in the vacuum. Then the relevant x and x' in Eq. (9) both approach infinity. Expression (11) is therefore proportional to $\theta(\omega - \epsilon_k - E)\theta(\mu - \omega)$. Taking into account that $\mu < E$ and $\epsilon_k > 0$, we see that the diamagnetic contribution to $\langle J_x \rangle$ is identically zero (to second order in $\vec{A}$).

The physical meaning of this result is very simple: to that order, as appears in Eq. (9), only the time-averaged ($\omega = 0$) part of the diamagnetic perturbation acts on the energy-conserving part $\hat{G}_\omega$ of the Green's functions. A time-independent potential does not induce electronic transitions; it leaves electrons in states below the Fermi level, from which they cannot escape into the vacuum. It is clear from this interpretation that this result must remain valid in the interacting system. We are left with

$$\langle J_x \rangle = \int \frac{d\omega}{2\pi}\frac{d^2k}{(2\pi)^2}\frac{e\hbar^2}{m}\left(\frac{\partial}{\partial x'} - \frac{\partial}{\partial x}\right) \times \frac{1}{4}\left(\frac{e\hbar k_y}{mc}\right)^2 \int dx_1 dx_2 a(x_1)a(x_2)$$

$$\times\{\hat{G}_{\vec{k},\omega}(x,x_1)\hat{\sigma}_z[\hat{G}_{\vec{k},\omega+\Omega}(x_1,x_2)+\hat{G}_{\vec{k},\omega-\Omega}(x_1,x_2)]$$

$$\times\hat{\sigma}_z\hat{G}_{\vec{k},\omega}(x_2,x')\}^+|_{x'=x=\infty}. \quad (13)$$

As has been shown above, $G^+_{\vec{k}\omega}(x_1,\infty)=0$. The $\{\}^+$ factor in the right-hand side of Eq. (13) reduces to

$$G^r_{\vec{k}\omega}(x,x_1)[G^+_{\vec{k},\omega+\Omega}(x_1,x_2)+G^+_{k,\omega-\Omega}(x_1,x_2)]G^a_{\vec{k},\omega}(x_2,x').$$

The condition that x and x' approach infinity imposes that this product is zero unless $\omega>E+\epsilon_k\geq E$, so that $\omega+\Omega>E>\mu$ and $G^+_{\vec{k},\omega+\Omega}(x_1,x_2)=0$. Writing down explicitly the θ-function dependences of $G^r_1G^a$ and $G^+_{\omega-\Omega}$, we get

$$\langle J_x\rangle=\int\frac{d\omega}{2\pi}\frac{d^2\vec{k}}{(2\pi)^2}\,\theta(\omega-\epsilon_{\vec{k}}-E)\theta(\mu-\omega+\Omega)\,\frac{1}{4}\left(\frac{e\hbar k_y}{mc}\right)^2$$

$$\times\int dx_1dx_2a(x_1)a(x_2)\frac{e\hbar^2}{m}\left(\frac{\partial}{\partial x'}-\frac{\partial}{\partial x}\right)[G^r_{\vec{k},\omega}(x,x_1)G^+_{\vec{k},\omega-\Omega}(x_1,x_2)G^a_{\vec{k},\omega}(x_2,x')]\,|_{x'=x=\infty}. \quad (14)$$

Equation (14) is the general expression of the photocurrent in our "pseudo-one-dimensional" noninteracting system. Several remarks can be made about it.

(i) It is completely equivalent to Eq. (5) of Schaich and Ashcroft,[6] it is simply one of the several equivalent expressions of the quadratic response to the photon field—i.e., of the three-current response function which is represented in Fig. 1. [Note that $G^{(2)+}$ is obtained by simply opening the diagram of Fig. 1 at the J_x vertex, and taking the Keldysh indices at the beginning and end of the resulting line to be, respectively, (+) and (−).]

(ii) Its physical meaning is obvious: an electron is excited by the field out of an occupied state (factor $G^+_{\omega-\Omega}$) into an empty state of energy ω. If it then has a transverse energy $\omega-\epsilon_k$ large enough for it to go out into the vacuum, it contributes to the photocurrent J_x, its weight being proportional to the probability *intensity* ($G^r_\omega G^a_\omega$ factor) for going from the solid to $x=+\infty$. The two-particle propagator G^rG^a contains what is described as the last two processes of the three-step model (propagation in the excited state and transmission through the surface), but, as we shall discuss in Sec. IV, these are confused with contributions related to what is called the optical-transition step.

(iii) Note that Eq. (14) does not make any assumption about the shape of the potential along x, in the solid or out of it. This means that image force effects can be taken into account in Eq. (14), as long as they appear via a one-body potential.[13] Moreover, our simplifying assumption of complete translational invariance along the surface can be dropped, and band effects in the (k_y,k_z) plane can be included: let us now assume simply that there is a lattice periodicity with lattice vectors $\vec{\rho}_a$, $\vec{\rho}_b$ in the plane of the surface, and that the wave functions of the electron eigenstates can be factorized[14] into $\psi_m(x,\rho)=u^{(n)}_{\vec{k}}(\rho)\phi_p(x)$, where $u^{(n)}_{\vec{k}}$ is a Bloch function labeled by a wave vector $\vec{k}$ of the first Brillouin zone and a band index (n). Replacing the space Fourier transform (8) by the Bloch transform

$$G^{(2)+}_{\vec{k}n}(x,x';\ \omega,\omega')=\int dt\,d^2\rho\,dt'd^2\rho'G^{(2)+}(\vec{r}t,\vec{r}'t')\times u^{(n)}_{\vec{k}}(\vec{\rho})[u^{(n)}_{\vec{k}}(\rho')]^*e^{-i(\omega t-\omega' t')}, \quad (15)$$

one straightforwardly obtains

$$\langle J_x\rangle=\sum_{nn'}\int\frac{d\omega}{2\pi}\int_{\text{1st zone}}\frac{d^2\vec{k}}{(2\pi)^2}\,\theta(\omega-\epsilon^{(n')}_{\vec{k}}-E)\times\theta(\mu-\omega+\Omega)\,|M_{nn'}|^2\times\frac{1}{4}\int dx_1dx_2a(x_1)a(x_2)\frac{e\hbar^2}{m}\left(\frac{\partial}{\partial x'}-\frac{\partial}{\partial x}\right)\times[G^r_{\vec{k}n'\omega}(x,x_1)G^+_{\vec{k}n,\omega-\Omega}(x_1,x_2)\times G^a_{\vec{k}n'\omega}(x_2,x')]\,|_{x'=x=\infty}, \quad (16)$$

where $M_{nn'}$ is the matrix element for optical interband transitions in the present model:

$$M_{nn'}=\frac{e\hbar}{mc}\int d^2\vec{\rho}\,u^{(n)*}_{\vec{k}}(\vec{\rho})\frac{\partial}{\partial y}u^{(n')}_{\vec{k}}(\vec{\rho}), \quad (16')$$

which, for simplicity, is often assumed to be independent of $\vec{k}$.

(iv) Equation (14) can be checked by applying it to the case of a free-electron solid and a step surface potential (Fig. 2), which has been studied by

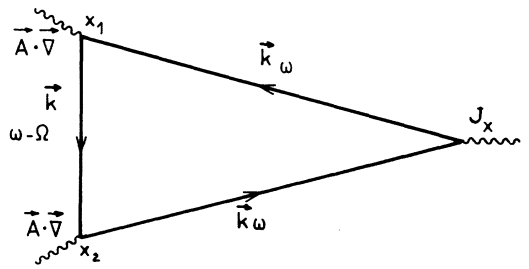

FIG. 1. Diagrammatic representation of the three-current response function.

several authors, and must give $\langle J_x \rangle = 0$ if the field is at normal incidence and if the x dependence of the vector potential is neglected (see, for instance, Ref. 6). The corresponding Green's functions are easily found by directly solving their equation of motion and matching at the surface:

$$G^{+}_{q,\omega-\Omega}(x,x') = \frac{2ik}{E}\, e^{-\kappa(x+x')} \qquad \text{for } x \text{ and } x' > 0$$

$$= \frac{4im}{\hbar^2 k} \sin kx \sin kx' - \frac{2i}{E}\left[\kappa \sin k(x+x') - k\cos k(x+x')\right] \qquad \text{for } x \text{ and } x' < 0$$

$$= \frac{2i}{E}\, e^{-\kappa x}(k\cos kx' - \kappa \sin kx') \qquad \text{for } x > 0,\ x' < 0 \qquad (17)$$

with

$$k = \left(\frac{2m}{\hbar^2}(\omega - \Omega - \epsilon_q)\right)^{1/2}, \quad \kappa = \left(\frac{2m}{\hbar^2}(E - \omega + \Omega - \epsilon_q)\right)^{1/2}, \qquad \omega - \Omega < \mu;$$

$$G^{r}_{q\omega}(x,x') = -\frac{2m}{\hbar^2 k_d} \sin(k_d x_<) e^{ik_d x_>} - \frac{2mi}{\hbar^2}\frac{e^{ik_d(x+x')}}{k_d + k_g} \qquad \text{for } x \text{ and } x' > 0$$

$$= \frac{2m}{\hbar^2 k_g} \sin(k_g x_>) e^{-ik_g x_<} - \frac{2mi}{\hbar^2}\frac{e^{-ik_g(x+x')}}{k_d + k_g} \qquad \text{for } x \text{ and } x' < 0$$

$$= -\frac{2mi}{\hbar^2}\frac{e^{i(k_d x - k_g x')}}{k_d + k_g} \qquad \text{for } x > 0,\ x' < 0 \qquad (18)$$

with

$$k_g = \left(\frac{2m}{\hbar^2}(\omega - \epsilon_q)\right)^{1/2}, \quad k_d = \left(\frac{2m}{\hbar^2}(\omega - \epsilon_q - E)\right)^{1/2}, \quad x_> = \max(x,x'), \quad x_< = \min(x,x'), \quad \omega - \epsilon_q > E.$$

Making use of Eqs. (17) and (18), and assuming in Eq. (14) that $a(x) = a = Cte$, one checks, after some tedious algebraic computation, that

$$a^2 \int dx_1 dx_2 \left(\frac{\partial}{\partial x'} - \frac{\partial}{\partial x}\right)\left[G^{r}_{q\omega}(x,x_1) G^{+}_{q,\omega-\Omega}(x_1,x_2) G^{a}_{q\omega}(x_2,x')\right]\Big|_{x'=x=\infty} = 0$$

so that the total current $\langle J_x \rangle = 0$.

(v) The energy distribution of the current can be defined immediately from Eq. (14). The analysis in energy of $\langle J_x \rangle$ measures the kinetic energy $\epsilon = \omega - E$ of the photoelectrons infinitely far from the solid. Setting $\langle J_x \rangle = \int_{-\infty}^{\infty} j(\epsilon)\, d\epsilon$, one gets from (14)

$$j(\epsilon) = \theta(\epsilon)\,\theta(\rho + \Omega - E - \epsilon)\,\frac{1}{2\pi}\int_{\epsilon_k=0}^{\epsilon_k=\epsilon}\frac{d^2k}{(2\pi)^2}\left(\frac{e\hbar k_y}{mc}\right)^2 \frac{1}{4}\int dx_1 dx_2 a(x_1)a(x_2)$$
$$\times \frac{e\hbar^2}{m}\left(\frac{\partial}{\partial x'} - \frac{\partial}{\partial x}\right)\left[G^{r}_{\vec{k},\epsilon+E}(x,x_1) G^{+}_{\vec{k},\epsilon-\Omega+E}(x_1,x_2) G^{a}_{\vec{k},\epsilon+E}(x_2 x')\right]\Big|_{x'=x=\infty}. \qquad (19)$$

(vi) Finally, it may be worthwhile to point out the formal difference between the photoemission and absorption response functions (which must be kept in mind when interpreting experiments). While $\langle J_x \rangle$ corresponds to a quadratic response (Fig. 1) involving a two-particle propagator in the final state, the optical absorption is obtained from a linear-response function (Fig. 3) with only a one-electron propagator in the final state. The physical implications of this difference will be developed in Sec. IV.

B. Interacting Systems

In a real solid, the electrons are involved in several types of interactions, e.g., electron-electron, electron-phonon, and electron-impurity scattering. As we have already pointed out in Sec. I, they are particularly important in photoemission, since the excited state of the electron lies at least several eV above the Fermi level μ, so that the mean free path in the final state is rather short (it may go down to ~ 10 Å in uv photoemission experiments). This shows up through three effects: first, the region of space from which the elastic photoelectrons (those which have suffered no energy loss) originate in a slab of thickness ~ l along the surface; on the contrary, in the independent-electron model, this escape depth is controlled by the field penetration depth

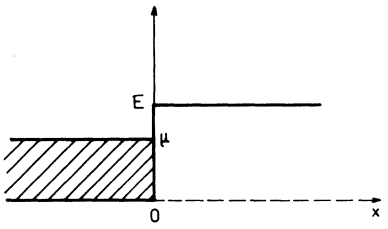

FIG. 2. Free-electron solid with step surface potential.

δ, which is usually much larger than l. Second, the final state is no longer a one-particle state, but a composite one made of a particle dressed with a large renormalization cloud. In other words, it corresponds to a rather poorly peaked spectral density. Finally, losses appear.

We must, therefore, now calculate the propagator $G^{(2)+}$ of Eq. (7) to second order in A and, in principle, to all orders in the internal interactions. Since the Dyson equation has the same formal expression in the matrix formalism as in the standard one, its perturbation expansion can be represented by Feynman diagrams. One simply has to keep in mind that products of propagators and self-energies are matrix products.

The diamagnetic part of H_1 does not contribute to $\langle J_x \rangle$ to order A^2, even in the presence of internal interactions, for the same physical reasons that were developed in Sec. II A.

The term in $\langle J_x \rangle$ of zeroth order in the internal couplings has been calculated in Sec. II A and is represented in Fig. 1. The terms of higher order are obtained by renormalizing this diagram to all orders in these couplings. One can separate all possible diagrams into four classes, three of which have a relatively simple physical meaning.

(i) Separate renormalizations of the bare diagram of Fig. 1. This corresponds to inserting in each of the three $\hat{G}$ matrices the self-energy corrections due to the internal interactions. The sum of all such diagrams is obtained by replacing in Eq. (14) or (16) bare $\hat{G}$'s by renormalized one-electron propagators, which we call $\hat{\mathcal{G}}$ and represent by double lines (Fig. 4).

(ii) Renormalization of the vertices of interaction with the external field (at points x_1 and x_2). It corresponds to diagrams in which, for instance, lines xx_1 and x_1x_2 are connected by one or more interaction lines. An example of such a term is

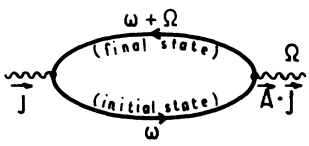

FIG. 3. Diagrammatic representation of the linear-response function for optical absorption.

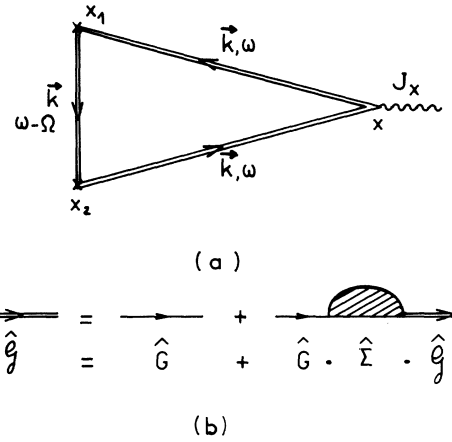

FIG. 4. (a) Three-current elastic response function. The double lines represent renormalized propagators. (b) Dyson equation for the renormalized propagator.

given in Fig. 5 for the case of electron-phonon interaction alone.

(iii) Renormalization of the J_x vertex, which corresponds to the diagrams in which lines xx_1 and xx_2 are connected by interaction lines. Such a term is schematically shown in Fig. 6, where conservation of the parallel momentum and of the energy has been taken into account.

(iv) Diagrams containing connections between the three $\hat{G}$ lines which cannot be cut into diagrams of type (ii) and (iii) by simply cutting two electron lines. An example of these is shown in Fig. 7. They can be expressed in terms of the irreducible vertex part with six electron lines, Γ_6.

Of course, the most general diagram is an arbitrary combination of these four independent types of renormalization.

We shall now try to make explicit the physical meaning of these various terms in the usual terminology of photoemission.

(i) Figure 4(a) describes a process in which an electron at energy $\omega - \Omega$, renormalized by the internal interactions, is excited by photon absorption up to a (renormalized) state at energy ω. The propagation of the escaping electron is represented

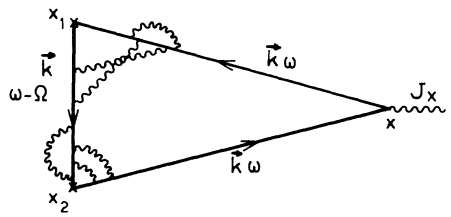

FIG. 5. An example of renormalization of the external field vertices by electron-phonon interaction.

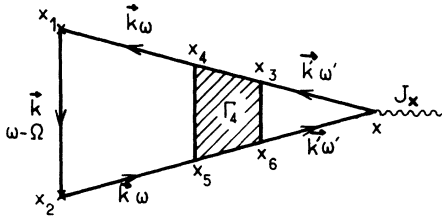

FIG. 6. Schematic representation of renormalization of the J_x vertex.

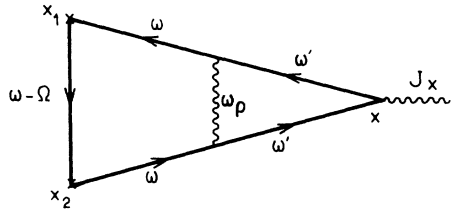

FIG. 8. An electron, excited from a deep state $(\omega-\Omega)$ to the primary state ω, creates a phonon of energy ω_p and leaves the solid at energy $\omega'=\omega-\omega_p$.

by the *two* ω lines. The interactions introduce self-energies, but the electron goes out at the same energy ω at which it has been first excited; therefore the corresponding current is elastic. In order for state $(\vec{k}, \omega)$ to contribute to $\langle J_x\rangle$, it must have a transverse energy $\omega-\epsilon_k>E$. We shall, from now on, neglect the self-energy corrections in the initial state $(\omega-\Omega$ line). It should, however, be kept in mind that they may be important in specific cases, among which are (a) experiments which measure the spin polarization of the photocurrent from magnetic metals. This situation has been analyzed by Anderson[15]; and (b) infrared catastrophy effects giving rise to asymmetrical broadenings in photoemission from deep initial states in metals.[16]

(ii) These terms (renormalization of the vertices of interaction with the external field) correspond to scattering between the "deep" hole, of energy $\omega-\Omega<\mu$, and the excited electron, of energy $\omega>E$, due to exchange of internal excitations. This is certainly a small effect if these excitations have energies much smaller than Ω (and *a fortiori* than $E-\mu$). This is the case for phonons, and we shall therefore neglect it in Sec. III. Electron-hole pairs can give non-negligible contributions, but the corresponding renormalization should vary slowly with energy ω, due to the fact that they have a regular continuous spectrum on the energy scale of interest (except possibly for $\Omega\sim\omega_{p1}$, the plasma frequency of the system).

(iii) On the contrary, renormalization of the J_x vertex can by no means be neglected. Indeed, the corresponding diagrams link two propagators at the energy of the excited state; i.e., they describe the history of the propagation of the excited electron. They give rise to the inelastic current, as can be seen on the simple diagram of this type (Fig. 8): an electron is excited from the deep state $(\omega-\Omega)$ up to the primary state ω, in which it creates a phonon[17] of energy ω_p, so that it goes out of the solid at energy $\omega'=\omega-\omega_p$ (if, of course, its transverse energy is still greater than E). Such excitation creations can be repeated; the resulting electron contributes to

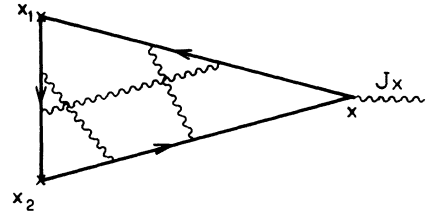

FIG. 7. An example of renormalization involving an irreducible Γ_6 vertex part.

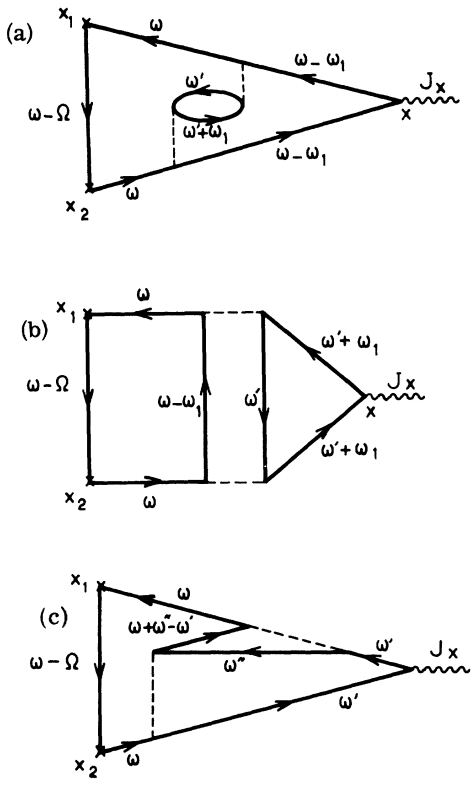

FIG. 9. Three diagrams involving a pair-excitation by Coulomb interaction. The contribution to $\langle J_x\rangle$ of the "primary" and of the "secondary" electrons are respectively depicted in (a) and (b).

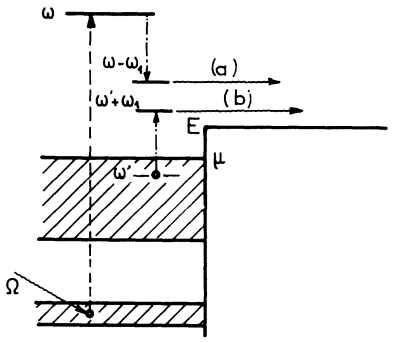

FIG. 10. Process of Figs. 9(a) and 9(b) in the energy-level representation.

$\langle J_x \rangle$ as long as it can escape. This class of terms also describes the emission of secondary electrons, which is induced by the electron-electron interaction. Figure 9(a) describes a process in which the primary electron goes out after having lost energy ω_1, which it has given to an electron-hole pair. Figure 9(b) describes the contribution to $\langle J_x \rangle$ due to the secondary electron, of energy $(\omega' + \omega_1)$, which has been excited in the same interaction process. Both effects are schematically depicted on Fig. 10. Fig. 9(c), which corresponds to a term of interference of the same order in the interaction, shows that the distinction between primary and secondary electrons is somewhat artificial (their contributions do not simply add). Finally, as pointed out by Langreth, [8] it would be incoherent (i.e., conservation of the number of particles would be violated) to keep self-energy corrections to $\hat{G}_\omega$ and to neglect Γ_4 corrections to $(\hat{G}_\omega \hat{G}_\omega)$. As we shall see in Sec. III, this implies that approximations used in calculating Σ and Γ_4 satisfy a consistency requirement.

(iv) Finally, the terms (see Fig. 7) which are not mere combinations of (i), (ii), and (iii) can be understood as three-particle correlation effects, i.e., interferences between the various elementary processes which come into play in the above effects. They cannot be reduced simply to any "step picture." Conservation laws bring in a coherence condition between these terms and Γ_4, as well as between Γ_4 and Σ.

It may be useful to note that each of these renormalization terms includes the contribution (at the corresponding order) of what is usually classified as indirect transitions. In fact the notion of indirect transition is particularly well adapted to the analysis of optical absorption, in which it can be used to calculate transition probabilities. In the case of photoemission, such a notion keeps a descriptive value, but its further use in calculations assumes that the step model be valid. Moreover, the presence of the surface cannot be ignored, especially when the electron mean free path is short. In the terminology of optical absorption, this gives rise to "nondirect" transitions, which simply means that the transverse wave vector is not a good quantum number. As shown by Schaich and Ashcroft and by Mahan, the corresponding "surface effect" does not simply add up to the "volume effect." This is clear in the microscopic formulation from the fact that all propagators have to be calculated in the presence of the surface.

At this point, one would like to calculate the above inelastic effects due to electron-electron scattering, since this mechanism is the leading one in most experimental cases. Unfortunately, the final-state energies in photoemission lie in a range[18] $(\omega - \mu > 4$ eV) in which the validity of the existing approximations is very questionable. (See, for instance, Beeferman and Ehrenreich's discussion of the optical absorption of metals[19].) Moreover, to our knowledge, the simplest of these approximations—namely, the RPA—cannot be performed to give analytical results for the self-energy in the case of a noninfinite medium. In those circumstances, it seems to us that electron-electron scattering effects can be taken into account in photoemission only by means of qualitative arguments, which can be founded on existing perturbation estimates of the corresponding scattering cross sections. [16]

We shall therefore limit ourselves, in the next section, to the case of electron-phonon scattering in a metal, where inelastic effects can be treated completely within reasonable approximations, and which permits to understand how the present formalism overlaps with semiphenomenological ones.

III. EFFECT OF ELECTRON-PHONON SCATTERING ON PHOTOEMISSION FROM A METAL

The reasons why we specialize in this section to the case of a metal are the following: in a metal, due to the screening effect of the gas of conduction electrons, electron-phonon interaction is at most of atomic range and can be assumed to be local. In an infinite metal, the self-energy is correctly described by Migdal's approximation, that is, in Keldysh's notation[9] [i.e., with the superscripts ij labeling, respectively, the lines and columns of the Keldysh matrix (4). In the following, + means 1 and − means 2].

$$\Sigma^{(ij)}_{\vec{k}\omega}(x,x') = ig^2(\sigma_z)_{ii}\int \frac{d\omega'}{2\pi}\,\frac{d^2k'}{(2\pi)^2} \times G^{(ij)}_{\vec{k}'\omega'}(x,x')D^{(ij)}_{\omega-\omega',\vec{k}-\vec{k}'}(x,x')(\sigma_z)_{jj}, \quad (20)$$

where g is the coupling constant. Equation (20) is represented by the diagrams of Fig. 11, where the wavy line represents a phonon propagator. As shown by Migdal, Σ is practically local in space

FIG. 11. Dyson equation for the self-energy in Migdal's approximation.

(its range is of atomic order), while it varies strongly with ω (on a scale of the order of the Debye frequency ω_D). Therefore, in such a uniform system,

$$\hat{\Sigma}_{\vec{k}\omega}(x,x') \cong \hat{\Sigma}(\omega)\,\delta(x-x'), \tag{21}$$

where $\hat{\Sigma}(\omega)$ is independent of position.

In our semi-infinite metal plus vacuum system Migdal's expression (20) remains valid (higher-order corrections are smaller by a factor $\sim \omega_D/\mu$) but the electron and phonon propagators are now those in the presence of the surface and of the vacuum. One can still safely assume Σ to be local, since this property derives from the fact that the phonon moves at the sound velocity, which is much smaller than the Fermi velocity characteristic of electron motion. We then assume that Eq. (21) becomes

$$\hat{\Sigma}_{\vec{k}\omega}(x,x') = \hat{\Sigma}(\omega)\theta(-x)\,\delta(x-x'), \tag{22}$$

i.e., that Σ has its bulk value everywhere inside the solid and is zero outside. This approximation, which follows the one made by Langreth in the impurity problem,[8] neglects the following effects:

In a real system, an electron in the vacuum may interact with the phonons by exciting a pair inside the solid (this is equivalent to saying that its image charge interacts with the phonons).

Inside the metal, $\hat{\Sigma}$ must vary with x in the vicinity of the surface for two reasons: on the one hand the phonon spectrum is perturbed in that region, in particular surface phonons generally appear. We shall ignore them in what follows.[20] On the other hand, as already noted, the interacting electron propagates in a semi-infinite system. Its propagator $\mathcal{G}(x,x')$ is the sum of two terms: the one corresponding to the direct path from x to x' gives the same contribution to $\hat{\Sigma}$ as in the infinite medium. The other one corresponds to a path going from x to x' with one reflection on the surface ($x=0$). It therefore contains a factor $e^{-|x+x'|/l}$, where l is the electron mean free path due to the phonons, and it gives an additional contribution to $\hat{\Sigma}$ in the region $-x<l$.

For all these reasons, our approximation only has a semiquantitative validity. Moreover, as we mentioned in Sec. IIB, we neglect the electron-phonon interaction in the initial state. This means that we forget about renormalization of the initial-state propagator and about the terms of classes (ii) and (iv) of Sec. IIB. Finally, we assume that the excited states ($\omega > E$) lie in a free-electron band and take for the surface potential the step approximation. The one-electron propagator $\mathcal{G}$ in an excited state is then easily calculated by including Σ in the equation of motion of G, solving separately for $x<0$ and $x>0$ and matching at the boundary. $\mathcal{G}^r_{\vec{q}\omega}$ ($\mathcal{G}^a_{\vec{q}\omega}$) is obtained from $G^r_{\vec{q}\omega}$ ($G^a_{\vec{q}\omega} = (G^r_{\vec{q}\omega})^*$) of Eq. (18) by the transformation

$$k_g \to k_g^r \quad (k_g^a = k_g^{r*}), \tag{23}$$

where

$$k_g^r \equiv k_{g_1} + ik_2 = \left(\frac{2m}{\hbar^2}\left[\omega - \epsilon_q - \Sigma^r(\omega)\right]\right)^{1/2}, \quad k_2 > 0.$$

The retarded component $\Sigma^r(\omega)$ of the self-energy is defined by

$$\Sigma^r(\omega) = \Sigma^c(\omega) + \Sigma^+(\omega) \equiv \Sigma^{(++)}(\omega) + \Sigma^{(+-)}(\omega), \tag{24}$$

where $\Sigma^{(ij)}$ is given by Eq. (20).

We are left with an expression for $\langle J_x \rangle$ which is simply a sum of two terms, namely: (a) the elastic current, represented by the diagram of Fig. 4(a), is immediately obtained from Eq. (14) or (16):

$$\langle J_x\rangle^{\mathrm{el}} = \int \frac{d\omega}{2\pi}\int \frac{d^2q}{(2\pi)^2}\,\theta(\omega-\epsilon_q-E)\theta(\mu-\omega+\Omega)\,|M|^2\,\frac{1}{4}\int dx_1 dx_2 a(x_1)a(x_2)$$
$$\times \frac{e\hbar^2}{m} G^+_{\vec{q},\omega-\Omega}(x_1,x_2)\left(\frac{\partial}{\partial x'}-\frac{\partial}{\partial x}\right)\left[\mathcal{G}^r_{\vec{q}\omega}(x,x_1)\,\mathcal{G}^a_{\vec{q}\omega}(x_2,x')\right]_{x'=x=\infty}. \tag{25}$$

With the help of Eqs. (23) and (18), this becomes

$$\langle J_x\rangle^{\mathrm{el}} = \frac{d\omega}{2\pi}\,\frac{d^2q}{(2\pi)^2}\left(-\frac{2iem}{\hbar^2}\right)|M|^2\,\theta(\omega-\epsilon_q-E)\,\theta(\mu-\omega+\Omega)$$
$$\times \int_{-\infty}^{0} dx_1 \int_{-\infty}^{0} dx_2 a(x_1)a(x_2)G^+_{\vec{q},\omega-\Omega}(x_1,x_2)\,\frac{k_d\cos[k_{g_1}(x_1-x_2)]}{(k_d+k_{g_1})^2+k_2^2}\exp[k_2(x_1+x_2)]. \tag{26}$$

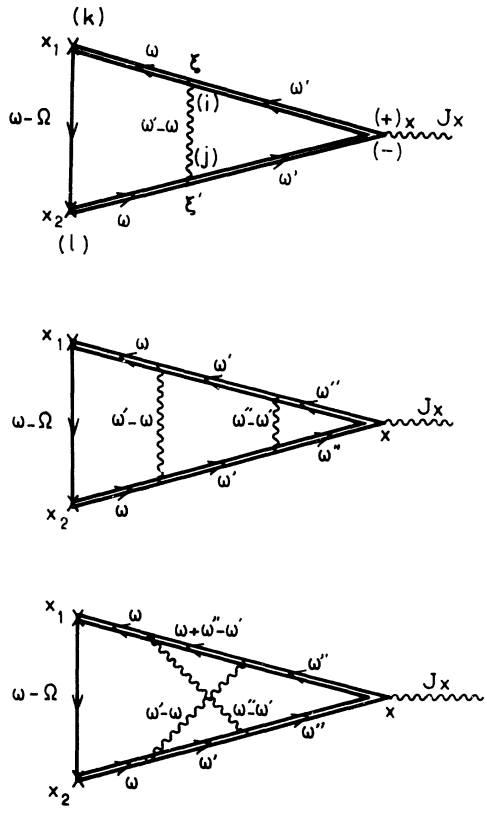

FIG. 12. One-phonon and two-phonon [(b) and (c)] terms in the renormalization of the J_x vertex. The term depicted in (c) is excluded when Migdal's approximation is retained for Σ.

In Eq. (26) we have taken advantage of the fact that, since $\omega - \Omega < \mu$, $G^{+}_{\omega-\Omega}(x_1 x_2)$ only has a range of atomic order in the vacuum; i.e., the contribution of occupied electron states in the vacuum can be neglected. Moreover, we have symmetrized it with the help of the general relation: $\hat{G}_{\omega}(\vec{r}_1, \vec{r}_2) = \hat{G}_{\omega}(\vec{r}_2, \vec{r}_1)$. In order to interpret Eq. (25) more easily and to simplify further calculations, we shall now assume that the system is pseudo-one-dimensional, that is, we shall forget about parallel momentum.[21] k_2 is then

$$k_2 = \mathrm{Im}\left|\frac{2m}{\hbar^2}\left[\omega - \Sigma^r(\omega)\right]\right)^{1/2}\Bigg| \tag{27}$$

and it is related to the mean free path $l(\omega)$ in the final state by $k_2 = 1/2l(\omega)$. The vector potential in the solid is $a(x) = a_0 e^{x/2\delta}$. It, then, appears in Eq. (26) that the electrons which contribute to the elastic EDC originate from a finite layer $-L(\omega) \lesssim x < 0$, of thickness

$$L(\omega) = \left(\frac{1}{\delta} + \frac{1}{l(\omega)}\right)^{-1} . \tag{28}$$

A more explicit expression of $\langle J_x \rangle^{\mathrm{el}}$ can be obtained only if one chooses a detailed model for the initial states, the properties of which appear in

$$G^{+}_{\omega-\Omega}(x_1, x_2) = 2i\pi \sum_m \varphi^*_m(x_1)\,\varphi_m(x_2) \times \delta(\omega - \Omega - \epsilon_m)\,\theta(\mu - \omega + \Omega), \tag{29}$$

where the φ_m's are the one-electron wave functions of the "deep" states. In order to illustrate our result, let us consider the simple case of an initial state with a completely localized electron at energy ϵ_0, viz.,

$$G^{+}_{\omega-\Omega}(x_1, x_2) = 2i\pi\,\delta(x_1 - x_2) \times \delta(\omega - \Omega - \epsilon_0)\,\theta(\mu - \omega + \Omega), \tag{30}$$

with $\epsilon_0 + \Omega > E$. We obtain

$$\langle J_x \rangle^{\mathrm{el}} = e\,\frac{2m}{\hbar^2}\,|M|^2\,\frac{k_d L(\epsilon_0 + \Omega)}{(k_d + k_{g_1})^2 + k_2^2}\; a_0^2 . \tag{31}$$

(b) The inelastic current is due to electrons which escape after having emitted one or more phonons. It corresponds to the terms (iii) of Sec. IIB (Fig. 6), in which the two ω lines are linked by one or more wavy lines. The one-phonon term is shown on Fig. 12(a); the two-phonon term may *a priori* contain either two nonintersecting wavy lines or two crossing lines [Figs. 12(b) and 12(c)]. However, in order for conservation laws to be satisfied, the following condition must be fulfilled: all the diagrams of the four-vertex part $\Gamma_4(\omega, \omega')$ (Fig. 6) are obtained by opening a bare electron line in any diagram of Σ, in all possible nonequivalent ways. Since Σ is given, in Migdal's approximation, by the sum of terms of Fig. 11,

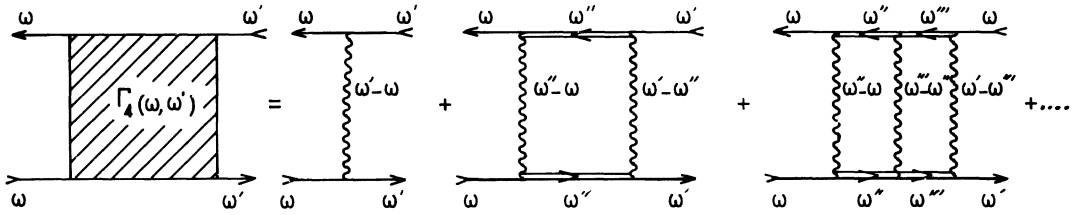

FIG. 13. Bethe-Salpeter equation for Γ_4 in Migdal's approximation.

one immediately finds that terms with crossing phonon lines [Fig. 12(c)] are excluded from Γ_4. For the same reason, no renormalization of the electron-phonon vertices appears, and Γ_4 reduces to the expression represented in Fig. 13. Let us now come back to the one-phonon term [Fig. 12(a)]. The fact that we are calculating $(\partial/\partial x' - \partial/\partial x) \times G^{(2)+}(x, x')$ (with $G^+ \equiv G^{(+-)}$), imposes that this diagram corresponds, in Keldysh's notation, to the contribution

$$\frac{e\hbar^2}{m}\,\frac{1}{4}\,|M|^2 ig^2 \sum_{ijkl=\pm} \int_{-\infty}^{0} dx_1 dx_2 d\xi d\xi' a(x_1)a(x_2)\left(\frac{\partial}{\partial x'} - \frac{\partial}{\partial x}\right)$$

$$\times[\mathcal{G}_{\omega'}^{(+i)}(x,\xi)(\sigma_z)_{ii} D_{\omega'-\omega}^{(ij)}(\xi,\xi')\mathcal{G}_{\omega}^{(jk)}(\xi,x_1)(\sigma_z)_{kk} G_{\omega-\Omega}^{(kl)}(x_1,x_2)(\sigma_z)_{ll}\mathcal{G}_{\omega}^{(lj)}(x_2,\xi')(\sigma_z)_{jj}\mathcal{G}_{\omega'}^{(j-)}(\xi',x')]_{x'=x=\infty}. \quad (32)$$

In order for such a term to be nonzero, we need that $\omega' > E$, which implies $\mathcal{G}_{\omega'}^{+} = 0$ and restricts the sum on i and j to $i = +$ and $j = -$. The only relevant element of the phonon propagator is therefore $D^{(+-)} \equiv D^+$, with

$$D_{\omega'-\omega}^{+}(\xi,\xi') = -2i\pi\lambda_{\omega'-\omega}(\xi,\xi')\theta(\omega-\omega'). \quad (33)$$

$\lambda_{\omega'-\omega}(\xi,\xi')$ is the phonon spectral density.[12] Equation (33), which is valid at $T = 0\,^\circ$K, implies that phonons can only be emitted: it imposes $\omega > \omega'$ in Eq. (32), i.e., the electron can only loose energy before escaping. Therefore $\omega > E$, and $\mathcal{G}_{\omega}^{+} = 0$. Expression (32) reduces to

$$\frac{e\hbar^2}{m}\,\frac{1}{4}\,|M|^2 ig^2 \int_{-\infty}^{0} dx_1 dx_2 d\xi\, d\xi' a(x_1)a(x_2)\left(\frac{\partial}{\partial x'} - \frac{\partial}{\partial x}\right)$$

$$\times[\mathcal{G}_{\omega'}^{r}(x,\xi)\mathcal{G}_{\omega}^{r}(\xi,x_1)G_{\omega-\Omega}^{+}(x_1,x_2)\mathcal{G}_{\omega}^{a}(x_2,\xi')\mathcal{G}_{\omega'}^{a}(\xi',x')D_{\omega'-\omega}^{r}(\xi,\xi')]_{x'=x=\infty}. \quad (34)$$

The same kind of analysis can be made on terms of higher order. It is found that, since phonon absorption cannot happen, the energies ω, ω', ω'', etc. [see Fig. 12(b)] of the excited electron lines can only decrease from left to right (in the triangular diagram representation).

One can then easily generalize expression (34) to include emission of 2, 3, etc. phonons; i.e., write the full Bethe-Salpeter equation for $\Gamma_4(\omega, \omega')$. In order to calculate it explicitly one must choose a definite model for the phonon spectrum. Since we are not dealing here with any specific solid, we shall use the simplest model, namely the Einstein one, in which phonons do not propagate and have a single frequency ω_0.[22] Then

$$D_{\omega}^{+}(\xi,\xi') = -i\pi\omega_0\theta(-\xi)\delta(\xi-\xi')\delta(\omega+\omega_0). \quad (35)$$

Setting $\Lambda = \pi\omega_0 g^2$, we then find for the inelastic current

$$\langle J_x\rangle^{\text{inel}} = \frac{e\hbar^2}{m}\,\frac{1}{4}\,|M|^2 \int\frac{d\omega'}{2\pi}\,\theta(\omega'-E)\int_{-\infty}^{0} dx_1 \int_{-\infty}^{0} dx_2 a(x_1)a(x_2)\left(\frac{\partial}{\partial x'} - \frac{\partial}{\partial x}\right)\left(\int_{-\infty}^{0} d\xi\,\mathcal{G}_{\omega'}^{r}(x,\xi)\mathcal{G}_{\omega'}^{a}(\xi,x')\right)_{x'=x=\infty}$$

$$\times\int\frac{d\omega}{2\pi}\,\theta(\mu-\omega+\Omega)\int_{-\infty}^{0} d\xi'\,\mathcal{G}_{\omega}^{r}(\xi',x_1)\,\mathcal{G}_{\omega}^{a}(x_2\xi')G_{\omega-\Omega}^{+}(x_1,x_2)F_{\omega'\omega}(\xi,\xi'), \quad (36)$$

with

$$F_{\omega'\omega}(\xi,\xi') = \theta(-\xi)\theta(-\xi')\Lambda \times[\delta(\xi-\xi')\delta(\omega-\omega'-\omega_0) + H_{\omega'\omega}(\xi,\xi')], \quad (37)$$

and H obeys the following integral equation:

$$H_{\omega'\omega}(\xi,\xi') = H_{\omega'+\omega_0}^{0}(\xi,\xi')\delta(\omega-\omega'-2\omega_0) + \int_{-\infty}^{0} d\xi''\,H_{\omega'+\omega_0}^{0}(\xi,\xi'')H_{\omega'+\omega_0,\omega}(\xi'',\xi'), \quad (38)$$

where

$$H_{\omega}^{0}(\xi,\xi') = \Lambda\mathcal{G}_{\omega}^{r}(\xi,\xi')\mathcal{G}_{\omega}^{a}(\xi',\xi).$$

Note that F, H, and H^0 are needed only in the region ξ and $\xi' < 0$. $F_{\omega'\omega}$ (or equivalently $H_{\omega'\omega}$) is the correlation function for an electron starting from ξ with energy ω and arriving at ξ' with energy $\omega' < \omega$. Since the phonons have a single frequency ω_0 the loss spectrum is discrete, $\omega' = \omega - n\omega_0$ ($n \geq 1$), so that

$$H_{\omega'\omega}(\xi,\xi') = \sum_{n=2}^{\infty} H_{\omega}^{(n)}(\xi,\xi')\delta(\omega-\omega'-n\omega_0) \quad (39)$$

with

$$H_\omega^{(n)}(\xi,\xi')=\int_{-\infty}^{0}d\xi_1\cdots\int_{-\infty}^{0}d\xi_{n-2}\times H^0_{\omega-(n-1)\omega_0}(\xi,\xi_1)\cdots H^0_{\omega-\omega_0}(\xi_{n-2},\xi'). \tag{39}$$

As is seen in Eq. (18) $\mathcal{G}^r$ (and $\mathcal{G}^a$) is a sum of two terms which correspond to direct and reflected waves. Following Langreth[8] we neglect in $\mathcal{G}^a\mathcal{G}^r$ the cross terms due to interferences between these waves, since they oscillate on less than an atomic distance and average to zero when surface inhomogeneities are taken into account. Then

$$H^0_\omega(\xi,\xi')=\left(\frac{2m}{\hbar^2}\right)^2\frac{\Lambda}{4\,|k_g^r|^2}\,(e^{-2k_2|\xi-\xi'|}+Re^{-2k_2|\xi+\xi'|}), \tag{40}$$

and the reflection coefficient R is given by

$$R=\left|(k_g^r-k_d)/(k_g^r+k_d)\right|^2 . \tag{41}$$

k_g^r, $k_2(=1/2l)$, and R in Eq. (40) are functions of ω. Because of this dependence, one cannot obtain a compact result for $H_\omega^{(n)}(\xi,\xi')$ for high n's. We therefore make one further approximation, which is to neglect in Eq. (39) the ω variation of H^0. This is quantitatively reasonable as far as we are concerned with losses $\omega-\omega'\ll\omega-E$, in which case R is quasiconstant, and $(\omega-\omega')/\omega\ll 1$ [variations of $\Sigma(\omega)$ are then small]. Our calculation will therefore hold for $n\ll(\omega-E)/\omega_0$.

Finally, calculating Σ from Eq. (20) in our model, we find that

$$\Sigma_2=-\operatorname{Im}\Sigma^r=\frac{m}{\hbar^2}\frac{\Lambda k_{g_1}}{|k_g^r|^2} . \tag{42}$$

Using this together with Eq. (27), one obtains

$$\left(\frac{2m}{\hbar^2}\right)\frac{\Lambda}{4\,|k_g^r|^2}=k_2 .$$

This relation, which ensures that the correlation function H^0 of Eq. (40) is correctly normalized, is a consequence of the consistency relation linking Σ and Γ_4.

$H^{(n)}$ is then calculated in the following way: consider the integral equation

$$f_\alpha(\xi,\xi')=H^0_\omega(\xi,\xi')+\alpha\int_{-\infty}^{0}d\xi_1 H^0_\omega(\xi,\xi_1)f_\alpha(\xi_1,\xi') . \tag{43}$$

Its solution is easily found to be

$$f_\alpha(\xi,\xi')=\left[\frac{(1+R)(1-\alpha)^{1/2}-(1-R)}{(1+R)(1-\alpha)^{1/2}+(1-R)}\times\exp\left(\frac{\xi+\xi'}{l}(1-\alpha)^{1/2}\right)+\exp\left(-\frac{|\xi-\xi'|}{l}(1-\alpha)^{1/2}\right)\right]. \tag{44}$$

Comparing Eq. (39) and the iteration expansion of $f_\alpha(\xi,\xi')$, one sees that $H_\omega^{(n)}(\xi,\xi')$ is the coefficient of the term in α^{n-2} in the expansion of $f_\alpha(\xi,\xi')$ in series of powers of α

$$H_\omega^{(n)}(\xi,\xi')=\frac{1}{(n-2)!}\left.\frac{\partial^{(n-2)}f_\alpha(\xi,\xi')}{\partial\alpha^{(n-2)}}\right|_{\alpha=0} .$$

This result is exactly equivalent to those found by Kane[2] and Duckett[3] by classical methods for slightly different problems. We rederive it in the Appendix by a simple random-walk calculation. Comparison of the above discussion with the random-walk formulation shows that the conditions for such a classical picture to be valid are that Migdal's approximation (or equivalent ones for other scattering mechanisms) holds; i.e., that vertex renormalization as well as renormalization of the phonon propagator may be neglected. If not, the simple expression of Fig. 13 for Γ_4 is no longer valid, and quantum interference terms appear in it which cannot be described classically. Also, the scattering center (here the phonon) does not propagate. If it does, the vertex function Γ_4 depends on four space variables instead of only two in the Einstein approximation, which again brings in quantum interferences between the propagating electron and the recoiling scatterer. These two conditions are fulfilled with sufficient accuracy in the cases of elastic impurity scattering in dilute alloys[8] and scattering by phonons (owing to the smallness of their velocity with respect to the electron one). But they are obviously not satisfied by electron-electron scattering, so that losses due to this mechanism are *not* described properly by the classical picture—i.e., by the knowledge of the single parameter $l(\omega)$.

The total current can now be rewritten as

$$\langle J_x\rangle=\int\frac{d\omega'}{2\pi}\int\frac{d\omega}{2\pi}\,\theta(\omega'-E)\,\theta(\mu-\omega+\Omega)A_{\omega\omega'} \tag{45}$$

and $A_{\omega\omega'}$, which gives the current contributed by electrons which have been excited from level $(\omega-\Omega)$ to ω, and escape after having lost $(\omega-\omega')$, is

$$A_{\omega\omega'}=\frac{e\hbar^2}{m}\int_{-\infty}^{0}dx_1\int_{-\infty}^{0}dx_2\,a(x_1)a(x_2)\tfrac{1}{4}\,|M|^2\times\frac{2m}{\hbar^2}\frac{(-2ik_d)}{|k_d+k_g^r|^2}G^*_{\omega-\Omega}(x_1,x_2)\times\cos[k_{g_1}(x_1-x_2)]e^{(x_1+x_2)/l}\delta(\omega-\omega')+\Lambda\int_{-\infty}^{0}d\xi\,\mathcal{G}^r_\omega(\xi,x_1)\mathcal{G}^a_\omega(x_2,\xi)\times\sum_{n=0}^{\infty}\varphi_n(\xi)\,\delta[\omega-\omega'-(n+1)\omega_0] , \tag{46}$$

$$\varphi_n(\xi)=\frac{1}{n!}\left.\frac{\partial^n\varphi(\alpha,\xi)}{\partial\alpha^n}\right|_{\alpha=0} ,$$

with

$$\varphi(\alpha,\xi)=\frac{2}{(1+R)(1-\alpha)^{1/2}+(1-R)}\times\exp\left(\frac{\xi(1-\alpha)^{1/2}}{l}\right). \tag{47}$$

The generating function $\varphi(\alpha,\xi)$ (which is the random-walk one) only describes the history of the excited electron *after the first phonon emmission*, as is shown by Eq. (46). What happens to that electron before this first emission is described by the quantity $\Lambda\mathcal{G}^r_\omega(\xi,x_1)\mathcal{G}^a_\omega(x_2,\xi)$, which reduces to the position correlation function if, and only if, points x_1 and x_2 can be taken to coincide. This is not generally the case, since $G^+_{\omega-\Omega}(x_1,x_2)$ is an oscillating function of x_1-x_2.

In the step model it is assumed that, once the electron has been excited, its further history is completely described by the (classical) position correlation function. Equation (46) shows that, on the one hand, optical excitation and propagation cannot be separated even in the elastic term (quantum interferences occur). This is discussed at length in Sec. IV. On the other hand, the knowledge of the correlation function is not sufficient to describe the electron behavior in the final state, except in two limiting "local" cases:
(i) the "deep" state lies in an extremely narrow band, then

$$G^+_{\omega-\Omega}(x_1,x_2)\propto\delta(x_1-x_2);$$

(ii) the final state is at very high energy (x-ray range). In that case the quantity $\mathcal{G}^r_\omega(x_1,\xi)\,\mathcal{G}^a_\omega(\xi,x_2)$ oscillates with (x_1-x_2) on much less than an atomic distance and, due to destructive interference, integration on (x_2-x_1) selects the region $x_2\simeq x_1$.

In order to put Eq. (46) into closer form, let us now specialize to the local case (i) of an infinitely narrow deep level at ϵ_0. Using Eq. (29), we obtain

$$A_{\omega\omega'}=\delta(\omega-\epsilon_0-\Omega)\sum_{n=0}^{\infty}A^{(n)}\delta(\omega'-\omega+n\omega_0),$$
$$A^{(n)}=e\,\frac{2m}{\hbar^2}\,|M|^2a_0^2\,\frac{k_d}{|k_d+k_g^r|^2}\,\phi_n, \tag{48}$$

where

$$\phi_n=\frac{1}{n!}\frac{d^n\phi(\alpha)}{d\alpha^n}\bigg|_{\alpha=0}$$

is the coefficient of α^n in the power expansion of

$$\phi(\alpha)=\frac{2}{(1+R)(1-\alpha)^{1/2}+(1-R)}\,\frac{l\delta}{l+\delta(1-\alpha)^{1/2}}. \tag{49}$$

In practice $\delta\gg l$, so that

$$\phi(\alpha)\simeq\frac{2l}{(1-\alpha)^{1/2}[(1+R)(1-\alpha)^{1/2}+(1-R)]} \tag{50}$$
$$=l\left(1+\alpha\,\frac{3+R}{4}+\alpha^2\,\frac{R^2+5R+10}{16}+\cdots\right).$$

The reflection coefficient R varies from $R=1$ (for $\omega=E$) to $R=0$ (for $\omega\gg E$). If $R\simeq1$, $\phi_n\simeq l$, therefore the contributions to J_x with $0,1,\ldots,n$ emitted phonons are comparable. If $R\simeq0$, $\phi_n\simeq l(2n+1)!/2^{2n}n!(n+1)!$ so that, for large n's, ϕ_n decreases as $1/\sqrt{n}$, i.e., quite slowly. It can be concluded that, in this case (pure electron-phonon scattering and narrow initial state), the high-energy part of the EDC would appear practically flat.

Finally, let us try to define extraction lengths. Since the correlation functions in the excited state with $0,1,\ldots,n$ emitted phonons are different for different n's, it is clear that, contrary to what is often assumed empirically, it is not physically meaningful to define a single extraction depth. One must define an extraction depth at given ω and ω', i.e., for a given primary excited energy and a given loss level. Moreover, we can define such quantities unambiguously only in the "local" cases—otherwise one cannot define a location for creation of the excited electron. For our narrow-deep-band model we set

$$\langle x\rangle_n=\psi_n/\phi_n,$$

with ψ_n the coefficient of α^n in the expansion of $\psi(\alpha)=\int_{-\infty}^{0}d\xi\,|\,\phi(\alpha,\xi)$, and $\langle x_n\rangle$ is the mean extraction depth for an electron at energy $\epsilon_0+\Omega-n\omega_0$, which has emitted n phonons.

We find

$$\langle x\rangle_0=l,$$
$$\langle x\rangle_1=l\left(\frac{5+R}{3+R}\right), \tag{51}$$
$$\langle x\rangle_2=l\left(\frac{R^2+7R+22}{R^2+5R+10}\right),\quad\text{etc.}$$

For $R\simeq0$, for instance, $\langle x\rangle_0=l$, $\langle x\rangle_1=5l/3$, $\langle x\rangle_2=11l/5,\ldots,\langle x\rangle_{n\gg1}\simeq(l/e)(\pi n)^{1/2}$. For finite R and large n's $\langle x\rangle_n\propto\sqrt{n}$, which is a well-known result for diffusion processes. Note that $\langle x\rangle_n$ depends on n (i.e., on $\omega-\omega'$) much more than on ω, which only appears via $l(\omega)$ and R.

From this it can be concluded that, in actual experimental situations, one can ascertain the region of space from where the contributing electrons originate only if the inelastic current can be neglected (as we shall see in Sec. IV, this means working in the high-energy part of the EDC). Otherwise, the measured EDC mixes an elastic contribution coming from a layer $l\lesssim x<0$, with a $n=1$ contribution coming from a layer -1, $6l\lesssim x<0$, etc., and these various terms generally cannot be separated.

Finally it can be remarked that the *relative* contributions to $\langle J_x\rangle$ of terms with $0,1,\ldots,n$ emitted phonons are independent of the coupling strength g (or of l) and are only given by geometrical fac-

tors. The variations of the coupling are compensated by those of the extraction lengths, which are proportional to l, so that $\langle J_x\rangle/l$ is—in this model—a constant.

IV. WHAT DOES PHOTOEMISSION MEASURE?

In this section we shall first discuss, in the light of the above results, the relevance of the step model, which is the basis of most interpretations of experiments. Let us recall that the step model makes two necessary assumptions: (a) absorption of the photon and propagation in the final state can be separated into independent (i.e., multiplicative) processes; (b) the absorption process appears in the expression of the photocurrent through the same quantity which appears in the absorption coefficient, namely the optical joint density of states (OJDS)

$$\rho(\omega,\Omega)=\sum_{\vec{k}nn'}|M_{nn'}(\vec{k})|^2\times\delta(\omega-\Omega-\epsilon_{\vec{k}}^{(n)})\,\delta(\omega-\epsilon_{\vec{k}}^{(n')}), \tag{52}$$

where n and n' are band indices for, respectively, the full and empty states of the (supposedly infinite) solid.

It is clear that the OJDS is a quantity appropriate only to a noninteracting system, since it involves only one-electron states. Let us first restrict to this case. As we have already pointed out in Sec. III, it is clear in Eq. (14) that the assumptions (a) and (b) are not strictly justified: indeed, if we try to factor out a quantity characteristic of propagation in the final state, it is most natural to choose the factor

$$\left(\frac{\partial}{\partial x'}-\frac{\partial}{\partial x}\right)G^r_{\vec{k}\omega}(x,x_1)G^a_{\vec{k}\omega}(x_2,x').$$

We are then left with another factor, which is simply $G^{\dagger}_{\vec{k},\omega-\Omega}(x_1,x_2)$, i.e., the Fourier transform of the spectral density of initial states. This is obviously not an "absorption factor", since it does not characterize the optical transition between two states, but only the initial one.

One would like to be able to separate out a factor $G^{\dagger}_{\vec{k},\omega-\Omega}(x_1,x_2)G^{-}_{\vec{k}\omega}(x_2,x_1)$, since

$$\rho(\omega,\Omega)=\frac{1}{L_x}\sum_{\vec{k}nn'}|M_{nn'}|^2\times\int dx_1dx_2G^{\dagger(n)}_{\vec{k},\omega-\Omega}(x_1,x_2)G^{-(n')}_{\vec{k}\omega}(x_2,x_1). \tag{53}$$

However, no simple relation exists, for a general system, which permits to express $G^r(x,x_1)G^a(x_2,x)$ as the product of $G^-(x_1,x_2)\,(=2\mathrm{Im}\,G^a)$ by some simple quantity related to a physical property of the system.[23]

The question can of course be raised of whether the photocurrent cannot, however, be proved to be approximately represented by the three-step expression and, if so, with what accuracy. Among the possible equivalent expressions of $\langle J_x\rangle$ in a noninteracting system, the one which is most illustrative for this purpose has been derived by Schaich and Ashcroft [Eq. (13) of Ref. 6]. It reads[24]

$$\langle J_x\rangle=\frac{2\pi e}{\hbar}\sum_{m,\tilde{u}}n(E_m)\times\left|\left\langle m\left|\frac{ie\hbar}{mc}\,\vec{A}\cdot\vec{\nabla}\right|\tilde{u}\right\rangle\right|^2\delta(E_m+\Omega-E_u). \tag{54}$$

$|m\rangle$ is a deep state with occupation function $n(E_m)$. The final state $|\tilde{u}\rangle$ is built so that it is the only one of the two degenerate eigenstates with given energy and parallel wave vector $\vec{k}$ having an outgoing plane-wave component at infinity in the vacuum.

The contribution of a given transition to Eq. (52) has a golden-rule-type of expression, but this expression does not actually verify the predictions of the step model. Indeed, the quantity

$$\left|\left\langle m\left|\frac{ieh}{mc}\,\vec{A}\cdot\vec{\nabla}\right|\tilde{u}\right\rangle\right|^2$$

contains information about the three steps. Information about the last two ones (propagation in the excited state and transmission through the surface) is included in it via the definition of state $|\tilde{u}\rangle$, which is an eigenstate of the solid *in the presence of the surface*. Its amplitude and structure (admixture of ingoing and outgoing Bloch states in the solid region) are determined, on the one hand, by matching conditions on the surface and, on the other hand, by the requirement that only outgoing waves in the vacuum contribute to photoemission. This information can clearly not be factored out of the matrix element, so that the optical-absorption step cannot be separated from the other two. This of course becomes even more impossible once the summation on all possible values of $\vec{k}$ has been performed.

One cannot therefore make a general prediction about the degree of accuracy with which the EDC may reproduce the OJDS of the (semi-infinite) solid, even in a noninteracting system. One expects that the important peaks or singularities of the OJDS will show up in the EDC, but the only possible way of comparing precisely the measurement of a specific EDC with a calculated band structure is to compute numerically Eq. (52) on the basis of the given band model applied to the semi infinite solid plus vacuum system. Let us emphasize that such a computation is much more heavy than that of the density of states of the infinite solid. It has been performed by Schaich and Ashcroft on model systems, and their results show that the EDC can differ considerably from the OJDS.

When scattering effects in the final state are included two problems arise in connection with the analysis of experiments: First, the elastic current (assuming that it can be measured separately) is affected by the scattering, so that Eq. (52) no longer describes it, and one has to come back to the general expression (25), in which the renormalized $\mathcal{G}$'s include self-energy effects. Equation (25) has no simple general expression in terms of one-electron wave functions and the $\mathcal{G}$'s must be calculated for each specific case. It can only be qualitatively argued that the final-state structures must be widened by an amount $\langle\Sigma'\rangle_\omega$ with respect to those of the noninteracting system [$\langle\Sigma'\rangle_\omega$ being some average of the imaginary part of the self-energy $\Sigma_{\vec{k}\omega}(x,x')$]. This appears in a particularly simple form in Eq. (31) (nonpropagating deep state and free-electron excited state).

The second problem is to know whether it is possible to separate in experiments the elastic current from the inelastic one. Such a separation is essential if one wants to make any—even only qualitative—interpretation of experimental results in terms of properties of the solid. If this is not done, the measured EDC at a given energy ω is, in general, due to electrons originating from a wide range of primary energies $\omega' > \omega$ (except if the deep state is a core level, in which case the width of the distribution of excited primary energies is due only to the photon line width. This can happen only in x-ray photoemission). Therefore such an EDC mixes contributions from densities of states in that whole energy range. Moreover, as shown in Sec. III, the outgoing electrons have various mean extraction depths depending on the losses they have experienced, so that they mix in generally unknown proportions surface and volume properties of the solid.

The essential scattering mechanisms are (a) electron-phonon interaction: in the interesting energy range the electron self-energy due to this mechanism alone is of the order of the Debye frequency $\omega_D \sim 10$–100 meV. This is also the order of magnitude of the average loss per phonon emission. (b) As shown by the existing perturbation estimates[25,26], as long as $\omega - \mu < 2\omega_{pl}$ (where ω_{pl} is the plasma frequency), the losses $\Delta\omega$ due to pair excitation are concentrated essentially in the region $\Delta\omega > \frac{1}{2}(\omega - \mu)$. For higher primary energies, plasmon emission can take place, and losses can be neglected only at most for $\Delta\omega < \omega_{pl}$. One can therefore approximately measure an elastic (with respect to losses by electron-electron interaction only) EDC, provided one studies the corresponding upper part of the EDC spectrum.

In order to make the above analysis slightly more practical, we shall now discuss what information about the solid can be reasonably extracted from EDC measurements depending on the energy of the primary excited electrons. As already stated, we discard the case of cesiated specimens and are interested only in materials with a clean surface, or possibly covered with a well-defined thin adsorption layer. The primary energy is then, in most cases, at least about 4 eV above the Fermi level.

(i) $4 \lesssim \omega - \mu \lesssim 10$ eV. This is most often realized with photoemission in the visible or near uv. If the material is a metal, the initial state lies in the conduction band; if it is a semiconductor it lies in the valence band. Although the mean free paths l_{ph} and l_{el} which would be due to, respectively, electron-phonon and electron-electron scattering alone can only be roughly estimated, it can be thought that $l_{el} \simeq l_{ph}$ for $\omega - \mu$ roughly of the order of 5 eV.[27]

In the region that we consider here, $\omega - E \lesssim 5$ eV. From what has been said above, the electrons which have lost energy by pair excitation are mostly concentrated at energies $\omega' < E$ (where they do not contribute to the EDC) or, for $\Omega \sim 10$ eV, at most at $\omega' \lesssim \omega - 3$ eV. Most of the EDC is therefore "electron elastic." It may of course by "phonon inelastic", i.e., contain contributions from electrons which have lost phonons before escaping. The electron-elastic current originates from a layer of thickness $\sim l_{el}$. On the other hand, as shown in Sec. III, an electron which has emitted n phonons has a mean extraction depth $\langle x\rangle_n \sim l_{ph}\sqrt{n}$. The EDC therefore contains phonon-elastic electrons as well as electrons which have emitted $n < n_0$ phonons, with $\langle x\rangle_{n_0} \sim l_{el}$. In practice, for $\omega - \mu \gtrsim 4$ eV, l_{el}/l_{ph} is at most a few units, and the broadening of the elastic EDC structure due to phonon losses is at most a few ω_D. Moreover, the presence of a self-energy in the final state, $\langle\Sigma'\rangle \sim \omega_D$, mixes contributions of one-electron states on a width $\Delta\omega \sim \omega_D$. One therefore expects structures with intrinsic widths typically of the order of a few tenths of eV.

Let us, however, insist that these structures do not necessarily reproduce those of the OJDS.

Note that in this regime l is typically ~ 100 Å; the relative weight of surface states is therefore small. However, the presence of surface defects or impurities may change non-negligibly the surface matching conditions in the excited state and thus modify the relationship between the OJDS and the measured EDC, which may consequently be rather sensitive to surface conditions (including the quality of the vacuum).

(ii) $15 \lesssim \omega - \mu \lesssim 40$ eV. This is realized in recent far-uv photoemission experiments.[28,29] In this regime l_{el} decreases rapidly with increasing $(\omega - \mu)$. It varies typically from $l_{el} \sim 15$ Å for $\omega - \mu \sim 15$ eV to $l_{el} \sim 5$ Å for $\omega - \mu \sim 30$ eV[30] (it reaches its minimum value for $\omega - \mu \sim 50$ eV, then

increases with ω at higher energies). On the other hand l_{ph} increases slowly with ω, so that $l_{el} \ll l_{ph}$. The electron-elastic current, which dominates $\langle J_x \rangle$ in the range $\omega_{max} - \omega \lesssim \omega_{pl}$ (where $\omega_{max} = \mu + \Omega$), is then at the same time essentially phonon elastic: its extraction depth is limited by $l_{el} \ll \langle x \rangle_0 < \langle x \rangle_1 < \ldots$, so that the probability p_n of extracting an electron which has emitted n phonons decreases rapidly with increasing n [using Eqs. (46) and (47) one shows that $p_1/p_0 \simeq \frac{1}{4}$, $p_n/p_0 \sim n^{-5/2}$ as $n \to \infty$]. The broadening of structures in the elastic EDC due to phonon losses is therefore negligible.

On the other hand, $\langle \Sigma' \rangle_\omega$ in the final states varies typically from ~ 1 eV for $\omega - \mu \sim 15$ eV to about 4 eV for $\omega - \mu \sim 30$ eV.[30] This implies that the true final state at energy ω mixes one-particle states from the whole energy range $|\omega' - \omega| \sim \langle \Sigma' \rangle \sim 1$–4 eV, which results in a considerable blurring out of the specific high-energy structures. It can therefore be expected that the corresponding EDC will reflect rather closely the accidents of the density of initial states alone.

Moreover, since, in this situation, $\omega - \mu$ is large compared with the pseudopotential in the solid, the surface matching conditions in the excited state have much less influence than in the visible or near-uv range. The presence of the surface is nevertheless crucial: because of the smallness of the extraction depth (at most a few atomic spacings) the relative weight of *initial* surface states is important and what is reflected in the elastic EDC is not the bulk density of states, but the one *close to the surface*. Ultraviolet photoemission therefore seems to be a promising tool for studying surface states, and especially chemisorbed ones, since these give rise to large resonancelike contributions. Such an effect has already been observed by Eastman and Cashion.[23]

(iii) $\omega \sim 1$ keV. This can happen only in soft-x-ray photoemission. [We only consider the case when initial states are not too deep (conduction or valence band).] In this regime the electron mean free path is limited by electron-electron scattering and is large (typically ~ 50 Å) so that the weight of surface states is negligible. Losses in the upper part of the spectrum are primarily due to plasmon emission.[31] One simplification can be made in this case: in Eq. (25) the final-state propagators can be approximated by those of an infinite free-electron gas. Indeed, they describe the one-dimensional motion of an electron with transverse energy $\omega - \epsilon_q$ much larger than the vacuum energy (except for a very small fraction $\lesssim (1/2\pi)(E/\omega)^{1/2}$ of the electrons which hit the surface at grazing incidence). Moreover, at such energies, band effects are completely negligible.

Since self-energy effects are negligible we can use the Schaich and Ashcroft expression (54) for $\langle J_x \rangle$. It is now extremely simple, because the final state $|\tilde{u}\rangle$ is a pure plane wave with positive transverse momentum (an optical transition takes place, and only this half of the excited free states contributes to $\langle J_x \rangle$ whose velocity is directed towards the vacuum). The surface conditions do not affect the matrix element, since the reflection coefficient $R = 0$. This is therefore the only case in which the step model is valid. The density of free-electron final states is regular and slowly varying, so that one expects that the elastic EDC will reflect closely the *bulk* initial-state structures.

From the above qualitative analysis it can be concluded that, while photoemission measurements in the visible range are very difficult to connect with simple properties of the emitting material, far-uv and x-ray photoemission, which are presently being developed, can provide valuable data:

uv experiments should give rather detailed information about (occupied) surface states;

x-ray experiments seem to be well adapted to explore bulk densities of (occupied) states.

ACKNOWLEDGMENTS

It is a pleasure to thank J. P. Hurault for his stimulating interest in this work, as well as C. Benoit à la Guillaume, B. Caroli, R. Combescot, M. Hulin, and P. Lavallard for various illuminating discussions.

APPENDIX: RANDOM-WALK CALCULATIONS OF SCATTERING EFFECTS

We recall here, as applied to our specific problem, the random-walk treatment developed by several authors[2,3] for studying the correlation function of the escaping electrons.

The model used has been defined in Sec. III: the excited electrons are in a free-electron band of a semi-infinite medium, they can excite Einstein phonons and loose a fixed energy ω_0 at each collision. For the surface potential, we retain the step approximation. The electron is excited and the effect of the surface is described through reflection and transmission coefficients, R and T. We shall restrain ourselves to a one-dimensional approximation which is sufficient to exhibit the qualitative results and simplifies appreciably the mathematical calculations.[32]

We shall compute the probability for a given electron emitted at the point $\xi_0 < 0$ in the solid to escape through the surface located at $\xi = 0$ after having suffered n collisions (i.e., emitted n phonons and lost energy $n\omega_0$).

For a one-dimensional infinite system we shall take the probability for an electron starting from ξ_0 to suffer its first collision between ξ and $\xi + d\xi$ under the form

$$p(\xi-\xi_0)d\xi=\frac{1}{2l}\exp\left(-\frac{|\xi-\xi_0|}{l}\right)d\xi\,, \tag{A1}$$

we assume as in Sec. III that the mean free path l and the reflexion and transmission coefficients R and T are energy independent in the relevant range.

Let us define the following functions: $G_n(\xi_0,\xi)d\xi$ $(\xi_0,\xi<0)$, which is the probability for an electron created at ξ_0 to suffer its nth collision between ξ and $\xi+d\xi$ without having ever reached the surface. $H_n(\xi_0,\xi)d\xi$ $(\xi_0,\xi<0)$, which is the probability for an electron created at ξ_0 and having been reflected on the surface between its $(n-1)$th and nth collisions to have suffered its $(n-1)$ first collisions in the negative half-space without having ever reached the surface and its nth collision between ξ and $\xi+d\xi$.

These functions obey the following recurrence relations:

$$\begin{aligned}G_{n+1}(\xi_0,\xi)&=\int_{-\infty}^{0}dy\,G_n(\xi_0,y)p(y-\xi),\\ H_{n+1}(\xi_0,\xi)&=\int_{-\infty}^{0}dy\,G_n(\xi_0,y)p(y+\xi),\quad \xi,\xi_0<0.\end{aligned} \tag{A2}$$

The probability for an electron to reach the surface for the first time after exactly n collisions is given by

$$P_n(\xi_0)=\int_{-\infty}^{0}d\xi' H_{n+1}(\xi_0,\xi'). \tag{A3}$$

We introduce the three generating functions

$$\mathcal{G}(\alpha,\xi_0,\xi),\quad \mathcal{K}(\alpha,\xi_0,\xi),\quad \mathcal{P}(\alpha,\xi_0).$$

They satisfy the following integral equations:

$$\begin{aligned}\mathcal{G}(\alpha,\xi_0,\xi)&=\delta(\xi-\xi_0)+\alpha\int_{-\infty}^{0}\mathcal{G}(\alpha,\xi_0,y)p(y-\xi)dy,\\ \mathcal{K}(\alpha,\xi_0,\xi)&=\alpha\int_{-\infty}^{0}\mathcal{G}(\alpha,\xi_0,y)p(y+\xi)dy,\\ \mathcal{P}(\alpha,\xi_0)&=(1/\alpha)\int_{-\infty}^{0}\mathcal{K}(\alpha,\xi_0,\xi')d\xi'.\end{aligned} \tag{A4}$$

With the simple form chosen for $p(y-\xi)$, we obtain easily

$$\begin{aligned}\mathcal{G}(\alpha,\xi_0,\xi)&=\delta(\xi-\xi_0)+\frac{\alpha}{2l(1-\alpha)^{1/2}}\\ &\quad\times\exp\left(-\frac{(1-\alpha)^{1/2}}{l}|\xi-\xi_0|\right)\\ &\quad+\frac{\alpha-2[1-(1-\alpha)^{1/2}]}{2l(1-\alpha)^{1/2}}\\ &\quad\times\exp\left(-\frac{(1-\alpha)^{1/2}}{l}|\xi+\xi_0|\right),\\ \mathcal{K}(\alpha,\xi_0,\xi)&=\frac{\alpha}{l[1+(1-\alpha)^{1/2}]}\\ &\quad\times\exp\left(-\frac{|\xi|+(1-\alpha)^{1/2}|\xi_0|}{l}\right),\\ \mathcal{P}(\alpha,\xi_0)&=\frac{1}{1+(1-\alpha)^{1/2}}\exp\left(-\frac{|\xi_0|}{l}(1-\alpha)^{1/2}\right).\end{aligned} \tag{A5}$$

When the electron reaches the surface it has a probability R to be reflected and $T=1-R$ to be transmitted. Therefore if it is transmitted the first time it reaches the surface, the corresponding generating function is $T\mathcal{P}(\alpha,\xi_0)$. If it is reflected it suffers anew collision in ξ_1, reaches the surface again, and is transmitted, the corresponding generating function is:

$$R\mathcal{K}(\alpha,\xi_0,\xi_1)T\mathcal{P}(\alpha,\xi_1)$$

The total generating function $\mathcal{L}(\alpha,\xi_0)$, which gives the probability for an electron to leave the metal after n collisions, is thus

$$\begin{aligned}\mathcal{L}(\alpha,\xi_0)&=T\mathcal{P}(\alpha,\xi_0)\\ &\quad+\int_{-\infty}^{0}R\mathcal{K}(\alpha,\xi_0,\xi_1)T\mathcal{P}(\alpha,\xi_1)d\xi_1\\ &\quad+\int_{-\infty}^{0}d\xi_1\int_{-\infty}^{0}d\xi_2 R\mathcal{K}(\alpha,\xi_0,\xi_1)T\mathcal{P}(\alpha,\xi_1)\\ &\quad\times R\mathcal{K}(\alpha,\xi_1,\xi_2)\,T\mathcal{P}(\alpha,\xi_2)+\cdots.\end{aligned} \tag{A6}$$

Using the explicit form of $\mathcal{P}$ and $\mathcal{K}$, we obtain[33]

$$\mathcal{L}(\alpha,\xi_0)=T\,\frac{\exp[-(1-\alpha)^{1/2}|\xi_0|/l]}{(1+R)(1-\alpha)^{1/2}+(1-R)}\,, \tag{A7}$$

an expression which is the equivalent of Eq. (47), which gives $\varphi(\alpha,\xi)$.

[1]W. E. Spicer, Phys. Rev. **112**, 114 (1958).
[2]E. O. Kane, Phys. Rev. **147**, 335 (1966).
[3]S. W. Duckett, Phys. Rev. **166**, 302 (1968).
[4]J. M. Ballantyne, Phys. Rev. B **6**, 1436 (1972).
[5]W. l. Schaich and N. W. Ashcroft, Solid State Commun. **8**, 1959 (1970)
[6]W. S. Schaich and N. W. Ashcroft, Phys. Rev. B **3**, 2452 (1971).
[7]G. D. Mahan, Phys. Rev. B **2**, 4334 (1970).
[8]D. C. Langreth, Phys. Rev. B **3**, 3120 (1971).
[9]L. V. Keldysh, Zh. Eksp. Teor. Fiz. **47**, 1515 (1964) [Sov. Phys.-JETP **20**, 1018 (1965)].
[10]This is not a serious restriction on the validity of the model, as long as one is interested in the total current or the EDC and not in the angular distribution of photoelectrons (see Ref. 7). In any case, a realistic calculation of this angular repartition would imply that one take into account not only the volume lattice structure but also the (often different) detailed arrangement of atoms in planes close to the surface.
[11]We shall systematically drop spin indices, since we shall not study in the following any magnetic effect.
[12]C. Caroli, R. Combescot, P. Nozières, and D. Saint-James, J. Phys. C **4**, 916 (1971).
[13]The image-potential approximation is known to be a good one except in a range of a few anströms close to the surface, where retarded and nonlocal effects become important.
[14]This last assumption is by no means necessary (see Ref. 6 or Sec. IV), but has the advantage of maintaining the relatively compact character of Eq. (14) while making optical interband transitions to appear explicitly, so that it is useful for qualitative discussion.
[15]P. W. Anderson, Philos. Mag. **24**, 203 (1971).
[16]S. Doniach and M. Šunjić, J. Phys. C **3**, 285 (1970).
[17]Since we are at $T=0\,^{\circ}\mathrm{K}$ and we assume the phonons to be at thermal equilibrium, phonon absorption processes are excluded

[18]We are discarding in this discussion the case of materials the extraction work of which would be reduced to very small values, since this is usually obtained by depositing on the surface a layer of a mixture of Cs and O. The composition and properties of such layers are presently poorly known, so that it is very difficult to predict how they can affect the photocurrent.

[19]L. W. Beeferman and H. Ehrenreich, Phys. Rev. B **2**, 364 (1970).

[20]This approximation should be improved on if one would need to study effects such as, for instance, losses due to vibrations of adatoms.

[21]This amounts to calculating the contribution to $\langle J_x \rangle$ of a given value of the parallel momentum, which has the same physical features as the true three-dimensional result.

[22]This assumption—which is coherent with the one made on the space variation of Σ—neglects the fact that surface atoms have, even in the Einstein model, a vibration frequency different from the bulk one.

[23]This would imply that G would satisfy a kind of optical theorem, which is known to hold only for the T matrix.

[24]This formula is obtained easily by developing the G's in Eq. (16) in terms of the three-dimensional wave functions of the solid plus vacuum system.

[25]E. O. Kane, Phys. Rev. **159**, 624 (1967).

[26]J. J. Quinn, Phys. Rev. **126**, 1453 (1962).

[27]The order of magnitude is about the same for a metal and a semiconductor since such excitation energies are much larger than a typical energy gap in a semiconductors.

[28]D. E. Eastman and W. D. Grobman, *Proceedings of the Eleventh International Conference on the Physics of Semiconductors* (Polish Scientific Publishers, Warsaw, 1972), Vol. 1, p. 889.

[29]D. E. Eastman, J. K. Cashion, Phys. Rev. Lett. **27**, 1520 (1971)

[30]R. Haydock, V. Heine, M. J. Kelly, J. B. Pendry, Phys. Rev. Lett. **29**, 868 (1972).

[31]See, for instance, K. Siegbahn, Philos. Trans. R. Soc. Lond. **A268**, 33 (1970).

[32]For three-dimensional calculation, sometimes referred to as the "Milne problem" see, Morse and Feshback, *Methods of Theoretical Physics* and Ref. 3.

[33]Expression (A6) reduces to a geometric series when the particular form (A1) of $p(\zeta - \zeta_0)$ is taken into account.